




COMPARING DIRECT CARBONATE AND STANDARD GRAPHITE ¹⁴C DETERMINATIONS OF BIOGENIC CARBONATES

Jordon Bright^{1*}  • Chris Ebert² • Matthew A Kosnik³ • John R Southon⁴ • Katherine Whitacre¹ • Paolo G Albano⁵ • Carola Flores^{6,7} • Thomas K Frazer⁸ • Quan Hua⁹  • Michal Kowalewski¹⁰ • Julieta C Martinelli¹¹ • David Oakley¹² • Wesley G Parker¹³ • Michael Retelle¹⁴ • Matias do Nascimento Ritter¹⁵  • Marcelo M Rivadeneira^{6,7,16} • Daniele Scarponi¹⁷ • Yurena Yanes¹³ • Martin Zuschin⁵ • Darrell S Kaufman¹

¹School of Earth and Sustainability, Northern Arizona University, Flagstaff, AZ 86011, USA

²Center for Ecosystem Sciences and Society, and Department of Biological Sciences, Northern Arizona University, Flagstaff, AZ, 86011, USA

³Department of Biological Sciences, Macquarie University, New South Wales 2109, Australia

⁴Keck Carbon Cycle AMS Laboratory, Department of Earth System Science, University of California at Irvine, Irvine, CA 92697, USA

⁵Department of Paleontology, University of Vienna, Althanstrasse 14, Vienna, Austria

⁶Centro de Estudios Avanzados en Zonas Áridas (CEAZA), Av. Ossandón 877, C.P. 1781681, Coquimbo, Chile

⁷Departamento de Biología Marina, Facultad de Ciencias del Mar, Universidad Católica del Norte, Av. Larrondo 1281, Coquimbo, Chile

⁸School of Natural Resources and Environment, University of Florida, Gainesville, FL 32611, USA

⁹Australian Nuclear Science and Technology Organisation, Locked Bag 2001, Kirrawee DC, NSW 2232, Australia

¹⁰Florida Museum of Natural History, University of Florida, Gainesville, FL 32611, USA

¹¹School of Fishery and Aquatic Sciences, University of Washington, Seattle, WA 98105, USA

¹²Department of Geosciences, Pennsylvania State University, University Park, PA 16802, USA

¹³Department of Geology, University of Cincinnati, Cincinnati, OH 45221, USA

¹⁴Department of Geology, Bates University, Lewiston, ME 04240, USA

¹⁵Centro de Estudos Costeiros, Limnológicos e Marinhos, Campus Litoral Norte, Universidade Federal do Rio Grande do Sul, Imbé, 95625-00, Rio Grande do Sul, Brazil

¹⁶Departamento de Biología, Universidad de la Serena, Av. Raul Bitrán 1305, La Serena, Chile

¹⁷Department of Biological, Geological and Environmental Sciences, University of Bologna, Piazza di Porta San Donato, I-40126 Bologna, Italy

ABSTRACT. The direct carbonate procedure for accelerator mass spectrometry radiocarbon (AMS ¹⁴C) dating of submilligram samples of biogenic carbonate without graphitization is becoming widely used in a variety of studies. We compare the results of 153 paired direct carbonate and standard graphite ¹⁴C determinations on single specimens of an assortment of biogenic carbonates. A reduced major axis regression shows a strong relationship between direct carbonate and graphite percent Modern Carbon (pMC) values ($m = 0.996$; 95% CI [0.991–1.001]). An analysis of differences and a 95% confidence interval on pMC values reveals that there is no significant difference between direct carbonate and graphite pMC values for 76% of analyzed specimens, although variation in direct carbonate pMC is underestimated. The difference between the two methods is typically within 2 pMC, with 61% of direct carbonate pMC measurements being higher than their paired graphite counterpart. Of the 36 specimens that did yield significant differences, all but three missed the 95% significance threshold by 1.2 pMC or less. These results show that direct carbonate ¹⁴C dating of biogenic carbonates is a cost-effective and efficient complement to standard graphite ¹⁴C dating.

KEYWORDS: biogenic carbonate, direct carbonate ¹⁴C AMS, standard graphite ¹⁴C AMS.

INTRODUCTION

An increasing variety of scientific investigations require a large number of radiocarbon analyses to address their underlying research questions, as exemplified by recent studies assessing the degree of time-averaging in natural or anthropological shelly accumulations (Kowalewski et al. 2018; New et al. 2019; Parker et al. 2019; Albano et al. 2020). These

*Corresponding author. Email: Jordon.Bright@nau.edu.

types of studies are generally constrained by their analytical budget rather than by the number of samples suitable for analysis, whereas some are limited by the size of the targeted specimens. This is true for a variety of sample types, including those based on biogenic carbonate. The standard graphite accelerator mass spectrometry radiocarbon (AMS ^{14}C) technique requires 8–10 mg of carbonate, which excludes dating individual small bivalve shells, for example. In response to this growing need, a direct carbonate AMS ^{14}C sputter method was developed by Longworth et al. (2013) that allows submilligram samples of carbonate powder to be analyzed quickly and efficiently. Several publications have highlighted the utility of direct carbonate ^{14}C dating where it has been used on its own or in combination with amino acid racemization to determine time-averaging in taphonomic studies (Dominguez et al. 2016; Kosnik et al. 2017; Ritter et al. 2017; Parker et al. 2019; Albano et al. 2020) or coupled with standard precision ^{14}C and uranium/thorium dating to determine coral age distributions (Grothe et al. 2016).

The direct carbonate AMS ^{14}C technique uses a cesium sputter source and a metal powder as a binder without the need to convert the carbonate sample to graphite but yields beam currents about an order of magnitude lower than the standard graphite method (Bush et al. 2013; Hua et al. 2019) which leads to the lower precision. Longworth et al. (2013) analyzed several materials with percent Modern Carbon (pMC) between 0.25 and 94.21. Using titanium powder, the direct carbonate method produced 1σ errors that ranged from 0.07 and 0.94 pMC, whereas 1σ errors on the same materials ranged from 0.08 and 0.87 pMC using graphite. Bush et al. (2013) analyzed numerous coral samples containing 0.10 to 89.06 pMC. Using iron powder, the direct carbonate method produced 1σ errors that ranged from 0.31 and 0.62 pMC, whereas 1σ errors on the same materials ranged from 0.03 and 0.11 pMC using graphite. Subsequent study by Hua et al. (2019) further established the utility of the direct carbonate technique, testing iron (Fe), niobium (Nb), and silver (Ag) powders before concluding that Nb powder was superior because it produced the highest beam current and lowest background.

Several studies have compared small numbers of paired direct carbonate and graphite ^{14}C results, showing that the two methods are comparable (Bush et al. 2013; Longworth et al. 2013; Kosnik et al. 2017; Kowalewski et al. 2018; Hua et al. 2019; New et al. 2019; Albano et al. 2020). In this paper, we have compiled a comprehensive dataset ($n = 153$) of published and unpublished direct carbonate and graphite ^{14}C determinations from biogenic carbonates belonging to several taxonomic groups (mollusks, corals, echinoderms, brachiopods) to further quantify any bias in the results based on the direct carbonate method.

MATERIALS AND METHODS

The carbonates featured in this study are all biogenic, as opposed to inorganically precipitated carbonate (e.g., limestone, speleothems). Samples comprise primarily aragonitic valves from the clams *Arctica islandica* (Linnaeus 1767), *Chamelea gallina* (Linnaeus 1758), *Codakia orbicularis* (Linnaeus 1758), *Corbula gibba* (Olivi 1792), *Dosinia caerulea* (Reeve 1850), *Mactra isabelleana* (d'Orbigny 1846), *Mulinia edulis* (King 1832), *Tawera spissa* (Deshayes 1835), *Tucetona pectinata* (Gmelin 1791), from open nomenclature species of the clams *Timoclea* and *Transennella*, from shells of the terrestrial snails *Actinella nitidiuscula* (Sowerby 1824) and *Polygyra septemvolva* (Say 1818), and from skeletal material of unidentified corals. As for the calcite polymorph, samples include valves from the brachiopod *Gryphus vitreus* (Born 1778) and plates from the sand dollars *Peronella peronii*

(Agassiz 1841) and *Leodia sexiesperforata* (Leske 1778). Several samples are shells that contain a mixture of aragonite and calcite polymorphs. These are the gastropods (limpets) *Fissurella maxima* (Sowerby 1834) and *Patella candei* (d'Orbigny 1840), the mussel *Choromytilus chorus* (Molina 1782), the cockle *Fulvia tenuicostata* (Lamarck 1819), the scallop *Argopecten purpuratus* (Lamarck 1819), and an open nomenclature species of the mussel *Modiolus*. References pertaining to the mineralogical composition of the biogenic material used in this study are provided in the Supplemental Information.

Ninety-three paired carbonate samples were processed at Northern Arizona University's (NAU) Amino Acid Geochronology Lab (AAGL) and NAU's Center for Ecosystem Science and Society (EcoSS) between 2015 and 2019. Most of the samples processed at NAU have been previously published (Kosnik et al. 2017; Oakley et al. 2017; Ritter et al. 2017; Kowalewski et al. 2018; Albano et al. 2020) and are detailed in the Supplemental Information.

Sample preparation at NAU followed protocols modified from Bush et al. (2013). Blanks, standards, and unknowns were sonicated in deionized distilled water (DDI water; 16.7 Mohm*cm), rinsed three times with DDI water, leached ~30% of their mass using 2N ACS grade hydrochloric acid to remove surface contaminants, and then finally rinsed three times with DDI to before being dried in a 50°C oven overnight. Samples for direct carbonate ¹⁴C analysis were ground to a fine powder using an agate mortar and pestle and manually mixed with 6.0–7.0 mg of metal powder in pre-baked (3 hr at 500°C) Kimble borosilicate glass culture tubes (6 mm OD × 50 mm). Samples processed at NAU before June 2018 were mixed with Fe powder (Alfa Aesar, -325 mesh, reduced, 98%) whereas samples processed after June 2018 were mixed with Nb powder (Alfa Aesar Puratronic, -325 mesh, 99.99%), following a change from Fe to Nb powders at the Keck Carbon Cycle AMS facility at the University of California, Irvine (UCI) in 2018. Powdered carbonate sample masses ranged between 0.30 and 0.50 mg, which equates to 36–60 µg of carbon, respectively. The culture tubes were flushed with N₂ gas to reduce contamination from atmospheric carbon and capped with Supelco plastic column caps (1/4" OD) until the carbonate-metal powder mixture was pressed into targets.

Samples processed at NAU for standard graphite AMS ¹⁴C analysis were graphitized at NAU's EcoSS lab following UCI protocols (sites.uci.edu/keckams/protocols). An aliquot of 7–8 mg of carbonate was placed in 13 × 75 mm BD Vacutainer plastic collection tubes (No. 366704). Ambient atmosphere was removed via vacuum before a small-bore needle was used to dispense 8 mL of ACS grade 85% phosphoric acid into each tube. The tubes were placed in a heating block at 70°C until the effervescence stopped. The evolved gas was removed via vacuum. Water vapor was removed by passing the gas through a mixture of liquid nitrogen and ethanol at approximately –80°C. Carbon dioxide was condensed to a solid using a liquid nitrogen bath and the remaining gasses were drawn off. The purified CO₂ was converted to graphite by reaction with Fe powder (Alfa Aesar, -325 mesh, reduced, 98%) in a hydrogen reducing environment at 550°C for 3 hr (Vogel et al. 1984).

The carbonate-metal or graphite-metal mixtures were pressed into pre-drilled (4.1-mm depth) aluminum targets at 400 psi, rotated 90°, and pressed again at 400 psi. Direct carbonate targets were pressed within 72 hr of powdering the first sample to minimize adsorption of CO₂. The IAEA C1 blank and IAEA C2 standard were pressed on the same day they were powderd. Limited testing reveals that powdered IAEA C1 and ¹⁴C-dead mollusk shell blanks can be kept

under N₂ for several days without adsorbing measurable amounts of CO₂ (see Results and Discussion). Targets were sent to UCI for AMS ¹⁴C analysis (Southon and Santos 2007).

We compiled 60 additional paired determinations generated at UCI or the Australian Nuclear Science and Technology Organisation (ANSTO) from Bush et al. (2011), New et al. (2019), Parker et al. (2019), and Hua et al. (2019). The respective publications provide the lab procedures and methods used for the additional paired determinations. Coauthors contributed all unpublished ages and previously unreported supporting information from UCI and ANSTO.

¹⁴C concentrations are given as pMC standard following the conventions of Stuvier and Polach (1977). Sample preparation backgrounds (procedural blanks) have been subtracted based on measurements of ¹⁴C-free calcite (IAEA C1 marble blank) using an isotope mixing calculation (Donahue et al. 1990). Procedural blanks for direct carbonate and standard graphite ¹⁴C determinations use powdered or graphitized IAEA C1, respectively. All graphite ¹⁴C determinations have been corrected for isotopic fractionation according to conventions of Stuvier and Polach (1977) with δ¹³C values measured on prepared graphite using the AMS spectrometer. These can differ from the δ¹³C values of the original material and are not provided.

Differences were calculated as “direct carbonate – graphite pMC,” with errors calculated in quadrature. The bivariate relationship between direct carbonate and graphite pMC values was evaluated using a reduced major axis regression (RMA) analysis. Unlike the classic ordinary least squares regressions (OLS), the RMA—also known as standardized major axis, geometric mean regression, or model II regression—minimizes the residual variation across both axes, not only the Y-axis, and hence accounts for measurement error in both axes (Quinn and Keough 2002; Smith 2009). The RMA regression avoids assumptions about the cause-and-effect between direct carbonate and graphite pMC values (Smith 2009). The PAST 4.03 statistical program (Hammer et al. 2001) was used for the RMA with 95% bootstrapped confidence intervals [N = 1999].

RESULTS AND DISCUSSION

Blank (IAEA C1) and Holocene Standard (IAEA C2) Performance

Graphite ¹⁴C analysis of NAU’s marble blank (IAEA C1) yields 0.44 ± 0.25 pMC (n = 8). Direct carbonate ¹⁴C analysis of NAU’s C1 blank yields 2.10 ± 0.33 pMC (n = 21) using Fe and 1.49 ± 0.66 pMC (n = 115) using Nb powder. Our direct carbonate blank results are similar to Hua et al. (2019) who demonstrated that Nb powder yields lower blanks than either Fe or Ag powders. The source of the direct carbonate ¹⁴C contamination in the NAU blank is unclear but likely stems from a variety of sources including, but not limited to, contamination during processing, carbon contamination in both the metal powders and the C1 powder itself, and uptake from atmospheric sources (Longworth et al. 2013). It is well known that powdered carbonate adsorbs atmospheric CO₂ over several years (Gagnon and Jones 1993) but it also rapidly adsorbs CO₂ after being baked at 500°C to oxidize indigenous and adsorbed carbon (Bush et al. 2013). A preliminary test conducted at NAU reveals that C1 powder mixed with Nb and stored in capped glass ampules under N₂ and then pressed immediately, pressed after four days, and pressed after nine days yields similar pMC (2.5 ± 0.4 (n = 2); 2.3 ± 0.3 (n = 4); 2.1 ± 0.2 (n = 2), respectively). A subsequent test used a ¹⁴C-dead *Rangia lecontei* (Conrad 1853) shell from the Early and Middle

Pleistocene Brawley Formation (Kirby et al. 2007). Targets pressed immediately after powdering and pressed after four and nine days storage under N_2 yielded similar pMC (1.7 ± 0.1 ($n = 4$); 1.6 ± 0.1 ($n = 4$); 1.8 ± 0.1 ($n = 4$), respectively). The small difference in pMC between the C1 blank and the *R. lecontei* blank is within the range of analytical variability of our C1 blank, thus, we contend that the marble and *Rangia* shell powders do not behave differently during processing. As standard practice, all direct carbonate ^{14}C blanks processed at NAU are pressed into targets on the same day they are powdering. Neither the marble nor the *Rangia* blanks suggest that adsorption of atmospheric CO_2 during processing is a significant source of contamination, unless it occurs almost instantaneously upon powdering. The metal powder itself is probably a larger source of carbon contamination (Bush et al. 2013; Hua et al. 2019) than is adsorption of atmospheric CO_2 .

Graphite ^{14}C analysis of NAU's Holocene carbonate standard (IAEA C2) yields 40.52 ± 0.74 pMC ($n = 7$). The C2 standard is consistent with the consensus value within 1σ error (41.14 ± 0.03 pMC; Rozanski et al. 1992). Direct carbonate ^{14}C analysis of NAU's C2 standard yields 41.30 ± 0.53 pMC ($n = 25$) using Fe powder and 40.70 ± 0.60 pMC ($n = 117$) using Nb powder. Both values are consistent with the consensus value within 1σ error (41.14 ± 0.03 pMC; Rozanski et al. 1992). Thus, there is evidence for extraneous young carbon contamination for the C1 and *R. lecontei* blanks (see previous section), but not for the C2 standard. Recently, Hua et al. (2019) demonstrated that the pMC of carbon contamination at ANSTO is similar to the C2 standard pMC. Thus, extraneous carbon contamination would be detectable in the C1 blank, but not in the C2 standard.

Key Differences between Direct Carbonate and Graphite ^{14}C Determination for Biominerals

Standard graphite ^{14}C processing involves dissolving biominerals in phosphoric acid followed by converting the resultant CO_2 to graphite. Negatively charged carbon ions are produced by sputtering a mixture of graphite and iron powder with cesium ions and then extracting the negatively charged carbon ions using an electric potential (Middleton 1983; Longworth et al. 2013). The direct carbonate ^{14}C method bypasses the graphitization process and uses cesium ions and an electrical potential to extract negatively charged carbon ions from powdered carbonate mixed with a metal powder.

The presence/absence of the acid dissolution step is a key difference between two methods and might have interesting implications regarding the sources of carbon measured by the two methods. Various studies suggest that mollusk shells (and other biominerals) contain a few tenths of a percent up to 5% by mass organic material, or “conchiolin” (Fremy 1855), which is an integral structural component within the biomineral (Galstoff 1964; Keith et al. 1993; Cuif et al. 2004; Zhang and Zhang 2006; Hadden et al. 2019). It is unlikely that the phosphoric acid dissolution of a biomineral during standard graphite ^{14}C processing oxidizes organic carbon to gaseous CO_2 . Converting the residual acid insoluble organics to CO_2 requires the use of a strong oxidizer like sodium persulfate (e.g., Mills and Quinn 1979; Hadden et al. 2019) or additional purification and combustion (e.g., Hadden et al. 2018). However, we are aware that the Cs sputtering of carbonate powder could liberate negative carbon ions from a shell's organic fraction. Non-graphitized organic material, such as charcoal and charred organics, do produce weak negative carbon currents when sputtered in the presence of a metal powder (e.g., Hedges et al. 1980; Bonani et al. 1984; Keller et al. 1984). Thus, we suspect that conchiolin-bound carbon could be an additional source of carbon present in direct carbonate ^{14}C measurements. Previous studies have

shown that paired shell and conchiolin ^{14}C ages (or ^{14}C activities) are similar (e.g., Berger et al. 1965; Burliegh 1983; Haynes and Mead 1987; Hadden et al. 2019). In some environments, however, organisms may preferentially incorporate significant amounts of ^{14}C -dead carbon in their conchiolin that is not present in their soft tissues or shell carbonate (Masters and Bada 1977; Hadden et al. 2018). We cautiously assume that small amounts of conchiolin in the biominerals featured in this study do not significantly influence the direct carbonate pMC values, but the topic deserves additional study.

Direct Carbonate versus Graphite pMC Determinations

We compiled pMC values from 153 individual carbonate specimens analyzed using both the direct carbonate and graphite ^{14}C techniques. Seventy-eight and 75 direct carbonate targets used Fe and Nb powder, respectively (Supplemental Information). Bush et al. (2013) concluded that the direct carbonate ^{14}C technique is less reliable for their oldest coral samples (> 30 ka BP), thus, their samples yielding ≤ 1.3 pMC using graphite are excluded in this comparison. One sample of *Maetra isabelleana* powder yielded strongly dissimilar graphite (78.5 pMC) and direct carbonate (105.7 pMC) results when analyzed seven months apart. Two samples of *Actinella nitidiuscula* material also produced strongly dissimilar graphite (0.91 and 0.36 pMC) and direct carbonate (2.0 and 2.5 pMC) results, respectively. The reason for the discrepancies is unclear. All three samples used Fe powder in the direct carbonate ^{14}C determinations. Two of the samples yield pMC values close to background and are therefore sensitive to contamination, and the third sample yielded pMC showing bomb ^{14}C contamination when analyzed with the direct carbonate technique whereas it did not when analyzed as graphite, thus, these three samples were excluded from further discussion. The remaining 150 specimens yield graphite and direct carbonate pMC values between 2.2 and 106.0 (see Supplemental Information).

Notably, the 1σ pMC analytical errors associated with the direct carbonate ^{14}C technique are typically two to eight times higher than for their graphite counterpart (Figure 1A). For samples that are late Holocene or younger in age, the larger uncertainty in the direct ^{14}C measurements is primarily derived from the combination of an order of magnitude lower beam currents (Bush et al. 2013; Hua et al. 2019) and the smaller number of replicate analysis ($0.5\times$) that the direct carbonate targets receive, compared to graphite targets. For early Holocene and older samples, the same sources of uncertainty apply but the dominant source of uncertainty becomes the large ($\pm 30\%$) uncertainty that is included in our blank correction. Typical precision (1σ error) in our direct carbonate ^{14}C compilation is less than 1.5% pMC for samples with pMC higher than 50 (Figure 1B), similar to the value reported by Hua et al. (2019). Given that the direct carbonate ^{14}C technique is a rapid and inexpensive survey method, this level of precision should be suitable for many research goals.

An RMA regression shows a strong relationship between direct carbonate and graphite pMC ($n = 150$) (Figure 2A). The slope of an RMA regression line is defined as the standard deviation of the y-axis values (direct carbonate pMC) divided by the standard deviation of the x-axis values (graphite pMC). The y-intercept is defined by the regression line passing through the bivariate centroid, or the point (\bar{x}, \bar{y}) , which here would be the mean of the graphite pMC values and the mean of the direct carbonate pMC values, respectively. The RMA regression using our entire compilation (Figure 2A) yields a slope near 1.000 (0.996 ± 0.003 ; 95% bootstrapped CI [N = 1999] of 0.991–1.001), and a y-intercept slightly above 0.00 (0.42; 95% bootstrapped CI [N = 1999] of 0.15–0.67) (Figure 1A). We observe slight differences in the RMA regression

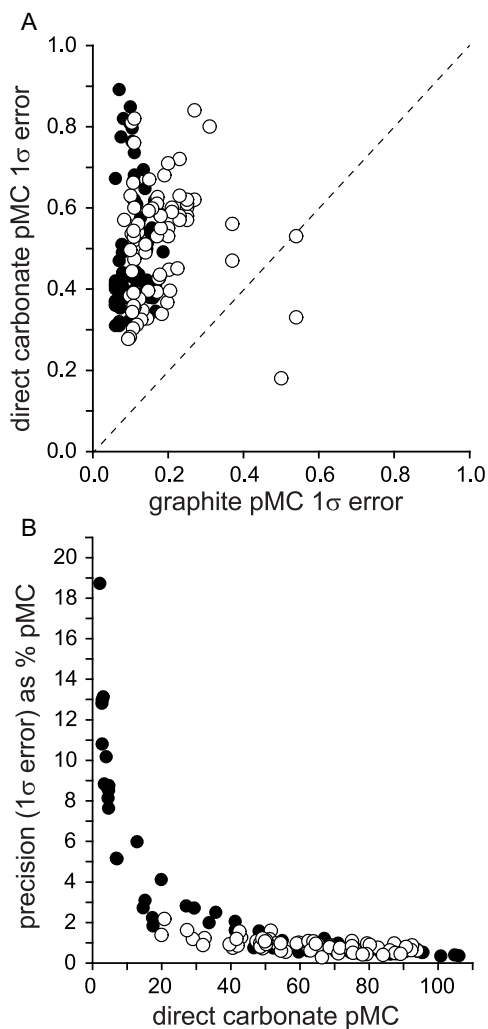


Figure 1 Cross-plots comparing analytical errors for direct carbonate and graphite pMC from the same biogenic carbonates. A—cross-plot of 1σ analytical errors produced by the graphite ^{14}C method versus the 1σ analytical errors produced by the direct carbonate ^{14}C method. Dashed line is a 1-to-1 line. B—cross-plot of direct carbonate ^{14}C pMC versus precision (1σ error) as a percentage of direct carbonate pMC. Solid black circles in both panels—Fe powder. Solid white circles in both panels—Nb powder.

results when the direct carbonate ^{14}C determinations using Fe and Nb are assessed individually (Figures 2B and 2C). Variability in the direct carbonate ^{14}C determinations using Fe powder is similar to that of their graphitized counterparts (i.e., RMA slope of 0.999 ± 0.003 ; Figure 2B). In contrast, the lower RMA slope of 0.988 ± 0.006 for the Nb-graphite pairs (Figure 2C) reveals that the direct carbonate ^{14}C determinations using Nb powder yield pMC values that are slightly less variable than their graphite counterparts. The difference in the Fe-only and Nb-only RMA regression slopes is small and overlap at 2σ errors. Thus, we contend that the differences in pMC values between the direct carbonate and graphite ^{14}C techniques is insignificant for most research goals.

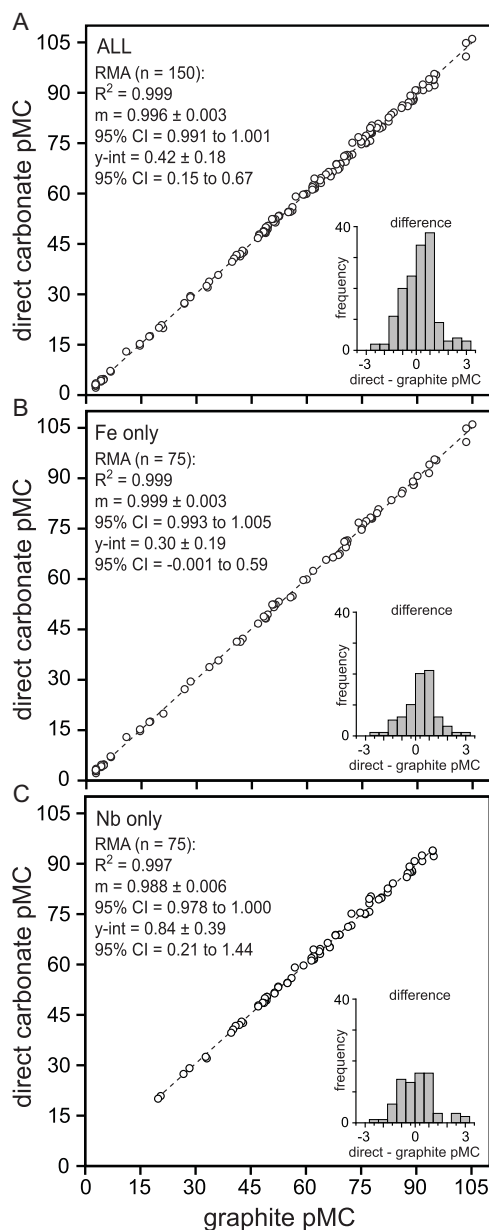


Figure 2 Reduced major axis (RMA) regression of paired direct carbonate and graphite pMC determinations. A—relationship using all data. B—relationship using iron (Fe) powder. C—relationship using niobium (Nb) powder. Analysis performed using PAST 4.03 statistical software (Hammer et al. 2001). Inset diagrams are frequency histograms of pMC differences, calculated as “direct – graphite pMC”.

The vast majority of direct carbonate pMC values are comparable to their graphite counterparts. Seventy-seven percent of differences are ± 1.0 pMC, and 94% percent are ± 2.0 pMC. Overall, we observe that 61% of direct carbonate pMC measurements are higher than their graphite counterpart (Figure 2A). When considered individually, however, 69%

of the direct carbonate ¹⁴C determinations using Fe yield positive differences whereas the direct carbonate ¹⁴C determinations using Nb yield differences that are more equally distributed, with 53% of the differences being positive (Figures 2B and 2C). The mean value of the differences is 0.19 pMC (95% CI: 0.04–0.34 pMC) for the entire compilation, indicating that the direct carbonate ¹⁴C technique yields pMC values slightly higher than the graphite technique. Much of the offset is contained in the direct carbonate determinations using Fe powder, however. When considered individually, the mean value of the Fe-graphite differences is 0.26 pMC (95% CI: 0.06–0.46 pMC), whereas the mean of the Nb-graphite differences is roughly half that, at 0.11 pMC (95% CI: –0.12–0.34 pMC). Dividing the differences by the direct carbonate pMC value yields a coefficient of variation of 0.9% (95% CI: –0.65% to 1.58%) for the entire compilation. When considered individually, the coefficient of variation for the Fe and Nb differences are 1.6% (95% CI: 0.3% to 2.8%) and 0.3% (95% CI: –0.3% to 0.6%), respectively. Collectively, this reveals a slight positive bias in direct carbonate ¹⁴C measurements relative to the graphite technique, with a more pronounced bias when using Fe powder.

The reason for the higher frequency of positive differences, especially when using Fe powder, (Figures 2A and 2B) and for why the two metal powders perform differently is unclear. One potential explanation is the adsorption of young atmospheric CO₂ during the powdering process (e.g., Kosnik et al. 2017). However, adsorption of CO₂ reasonably should affect all of the biomineral powders similarly, and not show a preference for the samples using Fe powder. Kosnik et al. (2017) suggested that perhaps the blank (marble) powder adsorbs CO₂ less efficiently than the biomineral powders, which would lead to excess adsorbed atmospheric CO₂ influence on biomineral pMC after blank subtraction. A blank under-correction of this sort should also affect the carbonate powders mixed with both metals similarly, rather than preferentially affecting the carbonate powders mixed with Fe (Figures 2B and 2C). Finally, we did not detect any adverse adsorption of atmospheric CO₂ in our blank marble powder or on ¹⁴C-dead mollusk shell powder after storage under N₂ for up to 9 days (see previous discussion of blank performance). Thus, adsorption of CO₂ during powdering does not adequately explain the higher tendency for positive differences when using Fe powder (Figure 2B). The discrepancy may be, in part, an artefact of the relatively small sample size (n=75). A more normal distribution in Fe-graphite differences might appear if the sample size was increased. It is also possible that the Fe powder imparts a slightly more frequent positive influence on the direct carbonate ¹⁴C pMC values. Recall in the earlier discussion of our C1 blank performance, we report that, on average, our C1 blank was about 0.7 pMC higher when using Fe powder than when using Nb powder. The blank correction process should remove contributions from both metal powders, however, rendering this an unsatisfactory explanation. And finally, the more equitable differences using Nb powder (Figure 2C) may be related to the improved beam current and reduced uncertainties when using Nb powder (Hua et al. 2019). We believe that our compilation is the largest of its kind, but it may still be too small to determine why there is a higher occurrence of positive differences when using Fe powder (Figure 2B).

With better counting statistics and less proportional background interference, direct carbonate pMC measurements on young samples tend to be indistinguishable from their graphite counterpart measurements as compared to older samples. The majority of the individual differences in our compilation (76%) are statistically indistinguishable at 95% CI (Supplemental Information). However, 36 of the differences (24%) do not meet this

criterion. These differences are evenly split between direct carbonate ^{14}C determinations using Fe powder ($n = 19$) and Nb powder ($n = 17$) (Table 1). Thirty-one of the 36 differences that do not include 0 at 95% CI are from samples that yield > 50 pMC as graphite, and the remaining five come from samples that yield < 50 pMC as graphite (Table 1). All five of the older samples yield differences that miss the 95% CI threshold by 0.5 pMC or less (Table 1). For the younger samples, 28/31 of the differences miss the 95% CI threshold by less than 1.2 pMC. The remaining three differences miss the 95% CI threshold by 1.3, 1.7, and 1.8 pMC (Table 1).

We acknowledge and caution that our study is limited to comparing the results of one direct carbonate and one graphite ^{14}C analyses per individual biomineral specimen. Several of the results compiled from Bush et al. (2013) comprise multiple analyses per coral specimen, but the overwhelming majority of our comparisons are based on single paired results (Supplemental Information). We calculated the weighted mean of the graphite and direct carbonate ^{14}C values (weighted by $1/\text{variance}$) and determined the number of biomineral specimens with 1σ analytical errors that overlapped the weighted mean. Ninety-three percent of the graphite pMC values overlap the weighted mean (versus the expected 68%), but only 45% of the direct carbonate pMC values overlap the weighted mean (versus the expected 68%). Thus, the reported uncertainty in the direct carbonate ^{14}C determinations underestimates the actual variance. We also suspect that some of the differences noted in this study may reflect slight variability between subsamples of a single biomineral specimen. Future comparative studies would benefit from analyzing each specimen multiple times with each AMS ^{14}C technique to more fully assess if there are statistically significant differences between the two techniques. Researchers typically only date a biomineral specimen once rather than multiple times, thus our study is more directly analogous to that approach. Keeping in mind that the direct carbonate pMC variance is underestimated and that we are using a single paired graphite and direct carbonate comparison per specimen, we contend that our study shows that the differences between the direct carbonate and graphite ^{14}C techniques is insignificant for most research goals.

We also observe a potentially interesting association between particular taxa and the differences that do not include 0 at a 95% CI. For example, the clams *Arctica islandica* (6/6 analyses) and *Modiolus* sp. (4/10 analyses), the sand dollar *Peronella peronii* (5/12 analyses), and the brachiopod *Gryphus vitreus* (3/6 analyses) appear to be disproportionately affected (Tables 1 and 2). The cause of this pattern is unclear. Carbonate mineralogy can be excluded because both aragonitic samples and calcitic samples populate the group (Table 1). Furthermore, some differences from the same taxon do include 0 at a 95% CI, for example, the remaining 3/6 *Gryphus vitreus* shells (Table 2). Thus, neither the organism (in a broader taxonomic sense) nor the carbonate mineralogy of the various skeletal materials is a satisfactory explanation. Using Fe or Nb powder for direct carbonate ^{14}C analysis does not explain why some taxa seem more affected than others (Table 1). The apparent patterns in Tables 1 and 2 may be an artifact of the small sample sizes per taxon, but it may hint that taxonomy or perhaps environmental variables specific to the habitat or life cycle of each taxon requires further consideration (e.g., Kosnik et al. 2017; Hadden et al. 2018). Larger sample sizes and additional tests are needed to better understand what may be causing differences between direct carbonate and graphite pMC determinations.

To further explore the relationship between the direct carbonate and graphite ^{14}C methods, the pMC differences shown in Figure 2A are plotted with respect to their respective taxonomic classifications in Figure 3. As noted previously in our discussion, the direct carbonate pMC

Table 1 Detailed breakdown of the taxa, generalized biological group, carbonate polymorph, standard graphite pMC values, direct carbonate metal powder, and pMC value of individual differences that exceed the 95% CI threshold.

Taxon	Group	Polymorph	Graphite pMC	Direct carbonate powder	Exceeds 95% CI (pMC)
<i>Actinella nitidiuscula</i>	Snail	Aragonite	10.9	Nb	0.53
<i>Argopecten purpuratus</i>	Scallop	Mixed	68.9	Fe	-0.18
<i>Argopecten purpuratus</i>	Scallop	Mixed	70.5	Fe	-0.10
<i>Arctica islandica</i>	Clam	Aragonite	50.5	Fe	0.89
<i>Arctica islandica</i>	Clam	Aragonite	50.9	Fe	0.65
<i>Arctica islandica</i>	Clam	Aragonite	51.4	Fe	0.13
<i>Arctica islandica</i>	Clam	Aragonite	55.5	Fe	-0.07
<i>Arctica islandica</i>	Clam	Aragonite	74.0	Fe	1.80
<i>Arctica islandica</i>	Clam	Aragonite	75.3	Fe	0.11
<i>Codakia orbicularis</i>	Clam	Aragonite	103.3	Fe	0.70
<i>Codakia orbicularis</i>	Clam	Aragonite	103.3	Fe	-1.72
Unidentified coral	Coral	Aragonite	2.6	Fe	0.25
<i>Corbula gibba</i>	Clam	Aragonite	94.7	Nb	-1.30
<i>Dosinia caerulea</i>	Clam	Aragonite	66.5	Nb	-0.26
<i>Dosinia caerulea</i>	Clam	Aragonite	77.2	Nb	-0.35
<i>Fissurella maxima</i>	Limpet	Mixed ^a	28.3	Nb	0.08
<i>Fissurella maxima</i>	Limpet	Mixed ^a	48.8	Nb	0.07
<i>Gryphus vitreus</i>	Brachiopod	Calcite	76.1	Nb	-0.24
<i>Gryphus vitreus</i>	Brachiopod	Calcite	87.4	Nb	-0.29
<i>Gryphus vitreus</i>	Brachiopod	Calcite	88.9	Nb	-0.36
<i>Leodia sexiesperforata</i>	Echinoderm	Calcite	104.9	Fe	0.30
<i>Modiolus</i> sp.	Mussel	Aragonite	52.3	Fe	0.14
<i>Modiolus</i> sp.	Mussel	Aragonite	61.6	Fe	0.04
<i>Modiolus</i> sp.	Mussel	Aragonite	76.1	Fe	0.45
<i>Modiolus</i> sp.	Mussel	Aragonite	79.4	Fe	0.32
<i>Mulinia edulis</i>	Clam	Aragonite	93.2	Fe	-0.38
<i>Patella candei</i>	Limpet	Mixed ^a	77.2	Nb	0.25
<i>Patella candei</i>	Limpet	Mixed ^a	88.1	Nb	0.19
<i>Peronella peronii</i>	Echinoderm	Calcite	57.0	Nb	1.01
<i>Peronella peronii</i>	Echinoderm	Calcite	62.1	Nb	1.17
<i>Peronella peronii</i>	Echinoderm	Calcite	72.4	Nb	1.17
<i>Peronella peronii</i>	Echinoderm	Calcite	77.2	Nb	0.83
<i>Peronella peronii</i>	Echinoderm	Calcite	77.7	Nb	1.15
<i>Polygyra septemvolva</i>	Snail	Aragonite	33.0	Nb	-0.43
<i>Transennella</i> sp.	Clam	Aragonite	77.2	Fe	0.06
<i>Tucetona pectinata</i>	Clam	Aragonite	59.0	Fe	0.06

^a“Mixed” refers to shells that contain both calcite and aragonite polymorphs.

Table 2 Summary of the taxa, sample size (n), generalized biological group, carbonate polymorph, number of differences that are statistically indistinguishable (SI) at 95% CI, and publication information for samples featured in this study.

Taxon	n	Group	Polymorph	SI	Reference
<i>Actinella nitidiuscula</i>	6 ^a	Snail	Aragonite	3/4	New et al. (2019)
<i>Argopecten purpuratus</i>	5	Scallop	Mixed	3/5	This study
<i>Arctica islandica</i>	6	Clam	Aragonite	0/6	This study
<i>Chamelea gallina</i>	1	Clam	Aragonite	1/1	This study
<i>Choromytilus chorus</i>	12	Mussel	Mixed ^b	12/12	This study
<i>Codakia orbicularis</i>	6	Clam	Aragonite	4/6	This study
Unidentified coral	20	Coral	Aragonite	19/20	Bush et al. (2011)
<i>Corbula gibba</i>	3	Clam	Aragonite	2/3	Albano et al. (2020)
<i>Corbula gibba</i>	2	Clam	Aragonite	2/2	This study
<i>Dosinia caerulea</i>	24	Clam	Aragonite	22/24	This study
<i>Fissurella maxima</i>	10	Limpet	Mixed ^b	8/10	This study
<i>Fulvia tenuicostata</i>	8	Cockle	Mixed ^b	8/8	Hua et al. (2019)
<i>Gryphus vitreus</i>	6	Brachiopod	Calcite	3/6	This study
<i>Leodia sexiesperforata</i>	1	Echinoderm	Calcite	0/1	Kowalewski et al. (2018)
<i>Mactra isabelleana</i>	1 ^a	Clam	Aragonite	0/1	Ritter et al. (2017)
<i>Modiolus</i> sp.	10	Mussel	Aragonite	6/10	This study
<i>Mulinia edulis</i>	5	Clam	Aragonite	4/5	This study
<i>Patella candei</i>	5	Limpet	Mixed ^b	3/5	Parker et al. (2019)
<i>Peronella peronii</i>	11	Echinoderm	Calcite	6/11	Kosnik et al. (2017)
<i>Polygyra septemvolva</i>	2	Snail	Aragonite	1/2	This study
<i>Tawera spissa</i>	1	Clam	Aragonite	1/1	Oakley et al. (2017)
<i>Timoclea</i> sp.	1	Clam	Aragonite	1/1	This study
<i>Transennella</i> sp.	4	Clam	Aragonite	3/4	This study
<i>Tucetona pectinata</i>	3	Clam	Aragonite	2/3	Kowalewski et al. (2018)

^aTwo analyses of *Actinella nitidiuscula* and one analysis of *Mactra isabelleana* yield widely different direct carbonate and graphite pMC values and are excluded from discussion and statistical analysis. See Supplemental Information.

^b“Mixed” refers to shells that contain both calcite and aragonite polymorphs.

values are more consistently higher than their graphite equivalents (Figure 3). Some biogenic carbonates might be prone to producing direct carbonate pMC values that are systematically offset from their graphite counterpart (Figure 3), although again, the sample sizes per taxon are admittedly small (1–24 individuals per taxon). The metal powder used in the direct carbonate ¹⁴C technique again does not appear to be a controlling factor at the taxonomic level (Figure 3). Note that the brachiopod *Gryphus vitreus* yields exclusively negative differences using Nb powder, the clams *Tucetona pectinata* and *Transennella* sp. yield exclusively positive differences using Fe powder, and the echinoderm *Peronella peronii* yields positive differences in nine of 11 analyses using Nb powder (Figure 3). Additional work is needed to determine whether the perceived taxonomic differences are real, for example if different taxa or perhaps different shells from different environments contain consistently different amounts of conchiolin with different ¹⁴C activities than the surrounding shell carbonate (Hadden et al. 2018), or whether the perceived differences are merely an artefact of small sample sizes.

cases, the direct carbonate ^{14}C technique yields pMC values from a variety of biogenic carbonates that are indistinguishable to pMC values produced using the more costly and time-intensive graphite ^{14}C technique. Thus, the direct carbonate ^{14}C technique is appropriate for a wide range of applications.

CONCLUSIONS

This study compared 153 individual biogenic carbonate samples from echinoderms, mollusks, brachiopods and corals that have been dated using both direct carbonate and graphite ^{14}C techniques. Three samples were excluded from discussion because their direct carbonate and graphite pMC values were strongly discordant. The remaining 150 samples range from 2.2 to 106.0 pMC. The direct carbonate ^{14}C technique produces 1σ pMC errors that are primarily two to 8 times higher than the associated graphite errors, and there is a weak negative correlation between the magnitude of the 1σ error differences and a sample's graphite pMC value. Our comparison of 150 paired direct carbonate and graphite ^{14}C determinations reveals a strong RMA regression relationship between the two techniques ($m = 0.996$; 95% CI [0.991–1.001]), and pMC values that are statistically indistinguishable from each other in 76% of the samples (at 95% CI). The variance in direct carbonate pMC values is underestimated, however. All but three of the direct carbonate ^{14}C determinations in this study were within 1.2 pMC of the 95% CI threshold of being statistically indistinguishable from their graphite equivalent. Some types of biogenic carbonates appear to produce direct carbonate pMC values that are consistently higher or lower than their graphite values, but sample sizes are small and the paired pMC values still statistically overlap in the vast majority of cases. The direct carbonate ^{14}C technique yields pMC values that overwhelmingly are indistinguishable from the standard graphite ^{14}C technique, but with the added benefit of more efficient laboratory preparation and processing.

ACKNOWLEDGMENTS

This study is a collaboration between the Amino Acid Geochronology Laboratory and the Center for Ecosystem Science and Society at Northern Arizona University, the Keck Carbon Cycle AMS Laboratory at the University of California-Irvine, and the Australian Nuclear Science and Technology Organisation.

This work is supported by grants NSF-1855381 (DSK), EAR-1559196 (DS), FONDECYT 3170913 (CF), FONDECYT 3160342 (JCM), FONDECYT 1140841, 1181300 and 1191452 (MMR), IODP/CAPES-091727/2014, and CNPq/MCTI-422766/2018-6 (MNR), EAR-1559196 (MK), NSF-1802153 (YY), and NSF-GRFP-1610397 (WGP). We thank Dan Cameron, Kathryn Geyer, and Aibhlin Ryan (NAU) for assisting with the direct carbonate ^{14}C samples. We thank Jenny E. Ross for providing the *R. lecontei* shell from the Brawley Formation, and both Austin Hendy (Natural History Museum of Los Angeles County) and Charles L. Powell, II, for assistance with the taxonomic references. Thoughtful comments from the Associate Editor Pieter Grootes and two anonymous reviewers greatly improved this manuscript.

SUPPLEMENTARY MATERIAL

To view supplementary material for this article, please visit <https://doi.org/10.1017/RDC.2020.131>

REFERENCES

- Agassiz L. 1841. Monographies d'Échinodermes vivans et fossiles. Échinites. Famille des Clypéasteroïdes. 2 (Seconde Monographie). Des Scutelles. Neuchâtel, Switzerland, i–iv, 1–151, pls 1–27.
- Albano PG, Hua Q, Kaufman DS, Tomašových A, Zuschin M, Agiadi K. 2020. Radiocarbon dating supports bivalve–fish age coupling along a bathymetric gradient in high-resolution paleoenvironmental studies. *Geology* 48:589–593. doi: [10.1130/G47210.1](https://doi.org/10.1130/G47210.1).
- Berger R, Fergusson GJ, Libby WF. 1965. UCLA radiocarbon dates IV. *Radiocarbon* 7:336–371. doi: [10.1017/S0033822200037310](https://doi.org/10.1017/S0033822200037310).
- Bonani G, Balzer R, Hofmann H-J, Morenzoni E, Nesi M, Suter M, Wölfli W. 1984. Properties of milligram size samples prepared for AMS ¹⁴C dating at ETH. *Nuclear Instruments and Methods in Physics Research B* 5:284–288. doi: [10.1016/0168-583X\(84\)90528-7](https://doi.org/10.1016/0168-583X(84)90528-7).
- Born I. 1778. Index rerum naturalium Musei Cæsarei Vindobonensis. Pars I.ma. Testacea. Verzeichniß der natürlichen Seltenheiten des k. k. Naturalien Cabinets zu Wien. Erster Theil. Schalthiere. [1–40], 1–458, [1–82]. Kraus: Vindobonae.
- Burleigh R. 1983. Two radiocarbon dates for freshwater shells from Hierakonpolis: Archaeological and geological implications. *Journal of Archaeological Science* 10:361–367. doi: [10.1016/0305-4403\(83\)90074-2](https://doi.org/10.1016/0305-4403(83)90074-2).
- Bush SL, Santos GM, Xu X, Southon JR, Thiagarajan N, Hines SK, Adkins JF. 2013. Simple, rapid, and cost effective: a screening method for ¹⁴C analysis of small carbonate samples. *Radiocarbon* 55:631–640. doi: [10.1017/S0033822200057787](https://doi.org/10.1017/S0033822200057787).
- Conrad TA. 1853. Descriptions of new fossils shells of the United States. *Journal of the Academy of Natural Sciences of Philadelphia* 2:273–276.
- Cuif J-P, Dauphin Y, Berthet P, Jegoudez J. 2004. Associated water and organic compounds in coral skeletons: Quantitative thermogravimetry coupled to infrared absorption spectrometry. *Geochemistry, Geophysics, Geosystems* 5: Q11011. doi: [10.1029/2004GC000783](https://doi.org/10.1029/2004GC000783).
- Cusack M, Parkinson D, Freer A, Perez-Huerta A, Fallick AE, Curry BB. 2008. Oxygen isotope composition of *Modiolus modiolus* aragonite in the context of biological and crystallographic control. *Mineralogical Magazine* 72:569–577.
- d'Orbigny AD. 1834–1847. Voyage dans l'Amérique méridionale (le Brésil, la République orientale de l'Uruguay, la République Argentine, la Patagonie, la République du Chili, la République de Bolivie, la République du Pérou), exécuté pendant les années 1826, 1827, 1828, 1829, 1830, 1831, 1832 et 1833, 5(3): Mollusques: i–xliv, 1–758, lám 1–85. Paris/Estrasburgo.
- d'Orbigny AD. 1839–1842. Mollusques, Echinodermes, Foraminifères et Polypiers recueillis aux Iles Canaries par MM. Webb et Berthelot et décrits par Alcide d'Orbigny. *Mollusques*. 117 p., pl. 1–7, 7B (p. 1–24 [Aug. 1839], 25–48 [Sept. 1839], 49–72 [Oct. 1839], 73–104 [Jan. 1840], 105–136 [Mar. 1840], 137–143 [Apr. 1840], 145–152 [Aug. 1842] pl. 1 [Jul. 1836], 2 [Dec. 1836], 3 [May 1842], 4–5 [June 1840], 7 [May 1842], 6,7B [Aug. 1842]. Béthune, Paris.
- Deshayes, GP, Milne-Edwards H. 1835. Histoire Naturelle des Animaux sans Vertèbres, présentant les caractères généraux et particuliers de ces animaux, leur distribution, leurs classes, leurs familles, leurs genres, et la citation des principales espèces qui s'y rapportent, par J.B.P.A. de Lamarck. Deuxième édition, Tome sixième. Histoire des Mollusques. iv + 600 pp. Paris: J. B. Baillière.
- Dominguez JG, Kosnik MA, Allen AP, Hua Q, Jacob DE, Kaufman DS, Whitacre K. 2016. Time-averaging and stratigraphic resolution in death assemblages and Holocene deposits: Sydney Harbour's molluscan record. *Palaios* 31:564–575. doi: [10.2110/palo.2015.087](https://doi.org/10.2110/palo.2015.087).
- Donahue DJ, Linick TW, Jull AJ. 1990. Isotope-ratio and background corrections for accelerator mass spectrometry radiocarbon measurements. *Radiocarbon* 32:135–142. doi: [10.1017/S00338222000040121](https://doi.org/10.1017/S00338222000040121).
- Dubois P. 2014. Calcification in echinoderms. In: Jangoux M, Lawrence JM, editors. *Echinoderm Studies* 3. Rotterdam: Balkema. p. 109–178.
- Fenger T, Surge D, Schone B, Milner N. 2007. Sclerochronology and geochemical variation in limpet shells (*Patella vulgate*): a new archive to reconstruct coastal sea surface temperature. *Geochemistry Geophysics Geosystems* 8: Q07001. doi: [10.1029/2006GC001488](https://doi.org/10.1029/2006GC001488).
- Flores C, Gayo EM, Salazar D, Broitman BR. 2018. δ¹⁸O of *Fissurella maxima* as a proxy for reconstructing Early Holocene sea surface temperatures in the coastal Atacama desert (25°S). *Palaeogeography, Palaeoclimatology, Palaeoecology* 499:22–34. doi: [10.1016/j.palaeo.2018.03.031](https://doi.org/10.1016/j.palaeo.2018.03.031).
- Fremy ME. 1855. Recherches chimiques sur les os. *Annales de Chimie et de Physique* 43:47–107.
- Gagnon AR, Jones GA. 1993. AMS-graphite target production methods at the Woods Hole Oceanographic Institution during 1986–1991. *Radiocarbon* 35:301–310. doi: [10.1017/S0033822200064985](https://doi.org/10.1017/S0033822200064985).
- Galstoff PS. 1964. The American Oyster *Crassostrea virginica* Gmelin. *Fishery Bulletin of the U.S. Fish and Wildlife Service* 64. 480 p.
- Gmelin JF. 1791. Vermes. In: Gmelin JF, editor. *Caroli a Linnaei Systema Naturae per Regna*

- Tria Naturae, Ed. 13. Tome 1(6). G.E. Beer, Lipsiae [Leipzig]. p. 3021–3910.
- Goetz AJ, Steinmetz DR, Griesshaber E, Zaefferer S, Raabe D, Kelm K, Irsen S, Sehrbrock A, Schmahl WW. 2011. Interdigitating biocalcite dendrites for a 3-D jigsaw structure in brachiopod shells. *Acta Biomaterialia* 7:2237–2243. doi: [10.1016/j.actbio.2011.01.035](https://doi.org/10.1016/j.actbio.2011.01.035).
- Grothe PR, Cobb KM, Bush SL, Cheng H, Santos G.M, Southon JR, Edwards RL, Deocampo DM, Sayani HR. 2016. A comparison of U/Th and rapid-screen ^{14}C dates from Line Island fossil corals. *Geochemistry, Geophysics, Geosystems* 17:833–845. doi: [10.1002/2015GC005893](https://doi.org/10.1002/2015GC005893).
- Hadden CS, Loftis KM, Cherkinsky A. 2018. Carbon isotopes ($\delta^{13}\text{C}$ and $\Delta^{14}\text{C}$) in shell carbonate, conchiolin, and soft tissues in eastern oyster (*Crassostrea virginica*). *Radiocarbon* 60:1125–1137. doi: [10.1017/RDC.2018.27](https://doi.org/10.1017/RDC.2018.27).
- Hadden, CS, Loftis KM, Cherkinsky A, Ritchison BT, Lulewicz IH, Thompson, VD. 2019. Radiocarbon in the marsh periwinkle (*Littorina irrorata*) conchiolin: applications for archaeology. *Radiocarbon* 61:1489–1500. doi: [10.1077/RDC.2019.53](https://doi.org/10.1077/RDC.2019.53).
- Hammer Ø, Harper DAT, Ryan PD. 2001. PAST: paleontological statistics software package for education and data analysis. *Palaeontologia Electronica* 4(1). 9 p. http://palaeo-electronica.org/2001_1/past/issue1_01.htm. Accessed version 4.03, June 30, 2020.
- Haynes CV, Jr, Mead AR. 1987. Radiocarbon dating and paleoclimatic significance of subfossil *Limicolaria* in northwestern Sudan. *Quaternary Research* 28:86–99. doi: [10.1016/0033-5894\(87\)90035-4](https://doi.org/10.1016/0033-5894(87)90035-4).
- Hedges REM, Wand JO, White NR. 1980. The production of C- beams for radiocarbon dating with accelerators. *Nuclear Instruments and Methods* 173:409–421. doi: [10.1016/0029-554X\(80\)90801-0](https://doi.org/10.1016/0029-554X(80)90801-0).
- Hua Q, Lavchenko VA, Kosnik MA. 2019. Direct AMS ^{14}C analysis of carbonate. *Radiocarbon* 61:1431–1440. doi: [10.1017/RDC.2019.24](https://doi.org/10.1017/RDC.2019.24).
- Jones CA. 2010. Mineralogy and seasonal growth of south Pacific mussel valves [MS thesis]. The University of Alabama, Tuscaloosa, Alabama. 73 p.
- Keith J, Stockwell S, Ball D, Remillard K, Kaplan D, Thannhauser T, Sherwood R. 1993. Comparative analysis of macromolecules in mollusc shells. *Comparative Biochemistry and Physiology B* 105:578–496. doi: [10.1016/0305-0491\(93\)90078-J](https://doi.org/10.1016/0305-0491(93)90078-J).
- Keller WA, Günter JR, Erne R. 1984. Preparation of elemental carbon for radiocarbon dating on the tandem accelerator. *Nuclear Instruments and Methods in Physics Research B* 5:280–283. doi: [10.1016/0168-583X\(84\)90527-5](https://doi.org/10.1016/0168-583X(84)90527-5).
- Kennedy WJ, Taylor JD, Hall A. 1969. Environmental and biological controls on bivalve shell mineralogy. *Biological Reviews* 44:499–530.
- King PP. 1832. Description of the Cirrhipeda, Conchifera and Mollusca, in a collection formed by the officers of H.M.S. Adventure and Beagle employed between the years 1826 and 1830 in surveying the southern coasts of South America, including the Straits of Magalhaens and the coast of Tierra del Fuego. *Zoological Journal* 5:332–349.
- Kirby SM, Janecke SU, Dorsey RJ, Housen BA, Langenheim VE, McDougall KA, Stealy AN. 2007. Pleistocene Brawley and Ocotillo Formations: evidence for initial strike-slip deformation along the San Felipe and San Jacinto Fault Zone, southern California. *The Journal of Geology* 115:43–62. doi: [10.1086/509248](https://doi.org/10.1086/509248).
- Kosnik MA, Hua Q, Kaufman DS, Kowalewski M, Whitacre K. 2017. Radiocarbon-calibrated amino acid racemization ages from Holocene sand dollars (*Peronella peronii*). *Quaternary Geochronology* 39:174–188. doi: [10.1016/j.quageo.2016.12.001](https://doi.org/10.1016/j.quageo.2016.12.001).
- Kowalewski M, Casebolt S, Hua Q, Whitacre KE, Kaufman DS, Kosnik MA. 2018. One fossil record, multiple time resolutions: Disparate time-averaging of echinoids and mollusks in a Holocene carbonate platform. *Geology* 46:51–54. doi: [10.1130/G39789.1](https://doi.org/10.1130/G39789.1).
- Lamarck J-BM de. 1819. Histoire naturelle des animaux sans vertèbres. Tome sixième, Ire partie. Paris: published by the author, vi + 343 p.
- Leske NG. 1778. Additamenta ad Jacobi Theodori Klein Naturalem Dispositionem Echinodermatum et Lucubratiunculam de Aculeis Echinorum Marinorum. 216 p.
- Linnaeus C. 1758. Systema Naturae per regna tria naturae, secundum classes, ordines, genera, species, cum characteribus, differentiis, synonymis, locis. Editio decima, reformata [10th revised edition], vol. 1: 824 p. Laurentius Salvius: Holmiae.
- Linnaeus C. 1767. Systema naturae per regna tria naturae: secundum classes, ordines, genera, species, cum characteribus, differentiis, synonymis, locis. Ed. 12. 1., Regnum Animale. 1 & 2. Holmiae, Laurentii Salvii. Holmiae [Stockholm], Laurentii Salvii. p. 1–532 [1766] p. 533–1327 [1767].
- Longworth BE, Robinson LF, Roberts ML, Beaupre SR, Burke A, Jenkins WJ. 2013. Carbonate as a sputter target material for rapid ^{14}C AMS. *Nuclear Instruments and Methods in Physics Research B* 294:328–334. doi: [10.1016/j.nimb.2012.05.014](https://doi.org/10.1016/j.nimb.2012.05.014).
- Masters PM, Bada JL. 1977. Racemization of isoleucine in fossil molluscs from Indian middens and interglacial terraces in southern California. *Earth and Planetary Science Letters* 37:173–183. doi: [10.1016/0012-821X\(77\)90162-5](https://doi.org/10.1016/0012-821X(77)90162-5).

- Middleton R. 1983. A versatile high intensity negative ion source. *Nuclear Instruments and Methods in Physics Research* 214:139–150. doi: [10.1016/0167-5087\(83\)90580-X](https://doi.org/10.1016/0167-5087(83)90580-X).
- Mills GL, Quinn, JG. 1979. Determination of organic carbon in marine sediments by persulfate oxidation. *Chemical Geology* 25:155–162. doi: [10.1016/0009-2541\(79\)90090-1](https://doi.org/10.1016/0009-2541(79)90090-1).
- Molina DJI. 1782. Compendio de la historia geografica natural y civil del Reyno de Chile. Primera parte. Madrid. 418 p.
- New E, Yanes Y, Cameron RAD, Miller JH, Teixeira D, Kaufman DS. 2019. Aminochronology and time averaging of Quaternary land snail assemblages from colluvial deposits in the Madeira Archipelago, Portugal. *Quaternary Research* 92:483–496. doi: [10.1017/qua.2019.1](https://doi.org/10.1017/qua.2019.1).
- Nielsen JK, Helama S, Rodland D, Nielsen JK. 2007. Eemian marine mollusks and barnacles from Ristinge Klint, Denmark: hydrodynamics and deficiency. *Netherlands Journal of Geoscience* 86:95–115.
- Oakley DOS, Kaufman DS, Gardner TW, Fisher DM, VanderLeest RA. 2017. Quaternary marine terrace chronology, North Canterbury, New Zealand, using amino acid racemization and infrared-stimulated luminescence. *Quaternary Research* 87:151–167. doi: [10.1017/qua.2016.9](https://doi.org/10.1017/qua.2016.9).
- Olivi G. 1792. *Zoologia Adriatica, ossia catalogo ragionato degli animali del golfo e della lagune di Venezia*. Bassano [G. Remondini e fl.]. [ix] + 334 + xxxii p., 9 pls.
- Parker WG, Yanes Y, Hernández EM, Hernández Marreno JC, Paris J, Surge D. 2019. Scale of time-averaging in archaeological shell middens from the Canary Islands. *The Holocene* 1–14. doi: [10.1177/0959683619883020](https://doi.org/10.1177/0959683619883020).
- Paul D, Mauldin R. 2013. Implications for Late Holocene climate from stable carbon and oxygen isotopic variability in soil and land snail shells from archaeological site 41KM69 in Texas, USA. *Quaternary International* 308–309:242–252. doi: [10.1016/j.quaint.2012.08.006](https://doi.org/10.1016/j.quaint.2012.08.006).
- Quinn GP, Keough MJ. 2002. *Experimental design and data analysis for biologists*. Cambridge University Press, Cambridge, UK. 537 p.
- Reeve LA. 1850. Monograph of the genus *Artemis*. In: Reeve LA, editor. *Conchologia iconica*. Vol. 6. London: L. Reeve & Co. p. 1–10.
- Ritter MN, Erthal F, Kosnik MA, Coimbra JC, Kaufman DS. 2017. Spatial variation in the temporal resolution of subtropical shallow-water molluscan death assemblages. *Palaios* 32:572–583. doi: [10.2110/palo.2017.003](https://doi.org/10.2110/palo.2017.003).
- Roger LM, George, AD, Shaw J, Hart, RD, Roberts M, Becker T, McDonald BJ, Evans, NJ. 2017. Geochemical and microstructural characterization of two species of cool-water bivalves (*Fulvia tenuicostata* and *Soletellina biradiata*) from Western Australia. *Biogeosciences* 14:1721–1737. doi: [10.5194/bg-14-1721-2017](https://doi.org/10.5194/bg-14-1721-2017).
- Rozanski K, Stichler W, Gofiantini R, Scott EM, Beukens RP, Kromer B, van der Plicht J. 1992. The IAEA ¹⁴C Intercomparison Exercise 1990. *Radiocarbon* 34:506–519. doi: [10.177/S00338222000063761](https://doi.org/10.177/S00338222000063761).
- Say T. 1818. Account of two new genera, and several new species, of fresh water and land snails. *Journal of the Academy of Natural Sciences of Philadelphia* 1:276–284.
- Smith RJ. 2009. Use and misuse of the reduced major axis for line-fitting. *American Journal of Physical Anthropology* 140:476–486. doi: [10.1002/ajpa.21090](https://doi.org/10.1002/ajpa.21090).
- Southon J, Santos GM. 2007. Life with MC-SNICS. Part II: further ion source development at the Keck Carbon Cycle AMS Facility. *Nuclear Instruments and Methods in Physics Research B* 259:88–93. doi: [10.1016/j.nimb.2007.01.147](https://doi.org/10.1016/j.nimb.2007.01.147).
- Sowerby GB, I. 1824. Descriptions, accompanied by figures, of several Helices, discovered by T. E. Bowdich, Esq. at Porto Santo. *Zoological Journal* 1(March):56–58.
- Sowerby GB, I, Sowerby GB, II. 1832–1841. *The conchological illustrations or, Coloured figures of all the hitherto unfigured recent shells*. London: privately published.
- Stuvier M, Polach HA. 1977. Discussion: reporting of ¹⁴C data. *Radiocarbon* 19:355–363. doi: [10.1017/S0033822200003672](https://doi.org/10.1017/S0033822200003672).
- Tschudin P. 2001. Shell morphology, shell texture and species discrimination of Caribbean *Tucetona* (Bivalvia, Glycymeridae). *Journal of Paleontology* 75:658–679.
- Vogel, JS, Southon, JR, Nelson, DE, Brown, TA. 1984. Performance of catalytically condensed carbon for use in accelerator mass spectrometry. *Nuclear Instruments and Methods in Physics Research* 223:289–293.
- Yanes Y, Al-Qattan NM, Rech JA, Pigati JS, Dodd JP, Nedila JC. 2019. Overview of the oxygen isotope systematics of land snails from North America. *Quaternary Research* 91:329–344. doi: [10.1017/qua.2018.79](https://doi.org/10.1017/qua.2018.79).
- Zhang C, Zhang R. 2006. Matrix proteins in the outer shells of molluscs. *Marine Biotechnology* 8:572–586. doi: [10.1007/s10126-005-6029-6](https://doi.org/10.1007/s10126-005-6029-6).